

# Acoustic softening – investigation of the volume effect and introduction of amplitude strafin parameter

Randy Cheng <sup>a,\*</sup>, Scott Rose <sup>b</sup>, Aflan Taub <sup>a</sup>

<sup>a</sup> Department of Material Science and Engineering, University of Michigan, Ann Arbor, MI, USA

<sup>b</sup> The Boeing Company, Saint Louis, MO, USA



## ARTICLE INFO

### Keywords:

Ultrasonic vibration  
Acoustic softening  
Acoustic energy  
Amplitude strafin  
Alumina alloy

## ABSTRACT

Acoustic softening is a phenomenon where metals exhibit a lower flow stress when excited by a vibration at ultrasonic frequencies. This softening effect has been well documented in the literature, however, there are two areas that require further in-depth analysis. The first relates to the wide range of reported softening responses for the same alloy. The second relates to the use of coefficients and compensation factors when modeling the acoustic softening phenomenon in a complex forming process. This study investigates the changes in softening response when altering specimen dimensions in ultrasonic assisted compression tests. Alumina alloy (AA) 2024-O and AA7075-O were machined to different dimensions and compressed with ultrasonic assistance, to investigate the relationship between specimen volume and softening response. An inverse relationship between softening magnitude and sample volume was found. When relating this to acoustic energy density and stress, the values are invariant because the standard acoustic equations cannot account for changes in specimen height. The amplitude strafin parameter, amplitude divided by the current specimen height, is introduced, and shown to account for changes in specimen dimensions. In addition, the softening effect diminishes relative to the state of strafin. The results suggest acoustic softening is a function of the amplitude strafin parameter and strafin history.

## 1. Introduction

Acoustic softening is a phenomenon in which material exhibits a lower flow stress when a vibration, typically above 20 kHz, is applied. An early study from Böhnhard and Langeneker showed that the shear stress in zinc single crystals decreased during ultrasonic excitation [1]. This proved to be a significant finding as the required energy input was lower than the requirement for thermal softening for an equivalent flow stress reduction. The proposed driving mechanism is a localization of acoustic energy at defect sites, such as dislocations, which lowers the critical energy required for slip. Some researchers have suggested this effect to be driven by material heating or simply the average stress during the unloading phase of the vibration, termed stress superposition; however, multiple studies have shown that sample heating does not reach hot forming temperatures [2–6] and the stress superposition cannot fully account for the reduction in flow stress [3,4].

Since this finding, acoustic softening has been demonstrated in a variety of metals and their alloys including alumina, copper, magnesium, titanium, and steel [6–10]. The ultrasonic vibration is often applied during the plastic regime for a short duration or infinite amount of

strafin and the change in flow stress can be represented by:

$$\sigma_f = \frac{\sigma_{UA}}{\sigma_{Control}} \quad (1)$$

$$\Delta\sigma = \frac{\sigma_{Control} - \sigma_{UA}}{\sigma_{Control}} \cdot 100 \quad (2)$$

where the softening fraction,  $\sigma_f$ , is the ratio of the flow stress for the ultrasonic assisted (UA) sample divided by the flow stress of the quasi-static loaded or control sample.  $\Delta\sigma$  is the softening magnitude which is the percent change in stress relative to the control sample. Acoustic variables such as acoustic energy density, intensity, and stress have been used to correlate  $\Delta\sigma$  and are represented by these equations:

$$E = \frac{\sigma_{acoustic} \omega \lambda}{c} = \rho \omega^2 \lambda^2 \frac{J}{m^3} \quad (3)$$

$$I = \rho c \omega^2 \lambda^2 \frac{W}{m^2} \quad (4)$$

\* Corresponding author.

E-mail address: [randyjfc@umich.edu](mailto:randyjfc@umich.edu) (R. Cheng).

$$\sigma = \omega \lambda \frac{\nabla}{\rho E_{\text{mod}}} [MPa] \quad (5)$$

$E$ ,  $I$ ,  $\sigma$  are the acoustic energy, fintensity, and stress terms respectively.  $\rho$  is the density of the sample,  $\omega$  is the angular frequency of the ultrasonic horn,  $\lambda$  is the applied amplitude,  $c$  is the maximum speed of sound in the sample, and  $E_{\text{mod}}$  is the elastic modulus of the workpiece. The acoustic stress and acoustic energy correlate to amplitude and amplitude squared, respectively.

Since amplitude is the main variable in ultrasonic assisted experiments, it is common to correlate the softening response to amplitude or amplitude to the power of a constant. The reported literature has been quite mixed in this correlation. Deshpande et al. performed ultrasonic assisted compression (UAC) on aluminum wire and found correlations to amplitude squared [11]. Wang et al. [12] observed a linear relationship to amplitude in ultrasonic assistance to tensile tests (UAT) of copper foils. Yao et al. [13] found UAC on commercially pure aluminum to correlate linearly to the amplitude. Sifidiq et al. [14] introduced  $U_{\text{soft}} = (1 - d \cdot I)^{e_{\text{ut}}}$ , where  $U_{\text{soft}}$  is the softening term,  $I$  is the acoustic intensity (Eq. (4)),  $d$  and  $e_{\text{ut}}$  are experimentally fitted constants; they used this equation to modify the initial slip resistance in crystal plasticity modeling of ultrasonic consolidation. Sifidiq et al. [15] later modeled other processes that used the same aluminum material but had to change the value of  $e_{\text{ut}}$  from 1 to 2.

In addition, the magnitude of softening reported for the same alloy can vary significantly. Several UAC examples on commercially pure aluminum are taken from literature. Daud et al. [3] observed a softening effect of 38% when using an amplitude of 10  $\mu\text{m}$ . Zhou et al. [7] achieved 37% softening with just a 4  $\mu\text{m}$  amplitude. Yao et al. [13] found a softening effect of 35% with only a 2  $\mu\text{m}$  vibration amplitude. Possible reasons for these differences include the state of strain of the sample at which the excitation was applied and differences in material microstructure. Sifidiq et al. [16] incorporated plastic strain using cold rolling and characterized the softening in UAC micro-indentation experiments; they observed a non-monotonic response for aluminum specimens. The three cited examples [3,7,13], apply ultrasonic vibration between strains of 0.15–0.20 and evaluates the softening at the very beginning. The strain states are fairly close for this sample set and likely contributes mainly to the variability. There are a few reports of grain size and texture impacting the softening response. Ahmad et al. [17] conducted ultrasonic assisted equal channel angular press on commercially pure aluminum with grain sizes ranging from 109  $\mu\text{m}$  to 1  $\mu\text{m}$  and discovered a direct correlation between softening and grain size. In contrast, Wang et al. [8] suggested an inverse relationship between grain size and softening in UAT of copper foils. Kang et al. [18] found that the sample texture has a direct relationship in differences of softening response when tensile testing copper sheet parallel or perpendicular to the rolled direction. Although microstructural differences can be a plausible explanation, a key difference in the cited studies is the size of the compression specimens. Daud's, Zhou's, and Yao's compression specimens had heights of 8 mm, 4 mm, and 2 mm respectively.

Aside from fundamental compression and tension experiments, acoustic softening has been tested on a variety of practical manufacturing processes. Vahdati et al. [19] included a vibration tool in single point incremental forming of straight grooves. The results showed greater strains were achieved due to acoustic softening and lower surface roughness. Cheng et al. [20] applied vibrations to two-point incremental forming, which uses a half-die as support. The forming force decreased by 18% and thickness reductions were measured to be greater than the applied amplitude of 3.2  $\mu\text{m}$ . Afzali and Lucas [21] demonstrated using ultrasonic vibrations in the press forming and showed a reduction of 22% with an applied amplitude of 20  $\mu\text{m}$ . Thus, there are a variety of applications demonstrated to benefit from flow stress reductions. However, the strategies on how to accurately model and predict the response require further work. Sedaghat et al. [22] presented a phenomenological model to simulate the expected forming in compression, punch forming, and incremental forming. To do so, they

used Kocks-Mecking's diffusion model where they lowered the activation energy for diffusions to overcome barriers. However, it was necessary to introduce two fitting constants for the punch and incremental forming simulations: effect coefficient and active volume parameter. The first coefficient accounts for the efficient transfer of energy from the transducer to the workpiece and the latter adjusts the active volume of material participating in slip. This poses an interesting situation for applying ultrasonic vibrations in deformation processes more complex than tension and compression. If a parallel comparison is drawn to hot forming, the higher the acoustic energy input into a finite material volume, the greater the softening response. Zhou et al. [7] initially demonstrated an inverse relationship between sample volume and acoustic softening magnitude in UAC. They accomplished this by reducing specimen height while maintaining a constant diameter. The main emphasis was on volume effects but the sample height was not further discussed. Sample height and softening correlated inversely.

This study further explores the relationship of specimen volume, height, and strain on the softening magnitude and discusses the implications for acoustic plasticity in complex forming processes. Two aluminum alloys, AA2024-O and AA7075-O are compressed with ultrasonic assistance to establish a relationship between acoustic softening response and amplitude. Sample dimensions are later modified to investigate the impact of acoustic softening on progressively smaller specimens. The results are plotted against common acoustic terms including acoustic energy density and acoustic stress.

## 2. Methods

### 2.1. Materials

Two aluminum alloys, AA2024-O and AA7075-O were supplied by The Boeing Company for this work. No additional heat treatment was performed as the material was already annealed. The starting sheet thickness is 1.60 mm and 3.18 mm for the AA2024-O and AA7075-O materials respectively. An electric discharge machine (EDM) was used to cut the samples into their appropriate dimensions listed in Table 1.

### 2.2. Experimental setup

The experimental setup was performed inside a cleanroom CNC machine, Fig. 1a, under displacement control. A Kistler dynamometer 9255A was used to measure the compressive forces during loading at a sampling rate of 40 Hz.

The ultrasonic transducer, highlighted in the orange box in Fig. 1a, operates similarly to welding and sonicating transducers where a stack of piezoceramic disks, Fig. 1b, respond to alternating current/voltage by mechanically driving. This generates an elastic wave that propagates to the tip of the transducer horn. The transducer operates at a frequency of 20 kHz and is powered by a Dukane generator model # 20VB480-2 L. A Polytec OFV 3001 vibrometer controller & OFV-3038 laser was used to measure the vibration amplitude of the horn. The stability of the transducer was verified by measuring the vibration amplitude at different loads; minimal difference was observed between the unloaded and loaded conditions. The compliance of the setup was measured before compression experiments by loading the flat tool against the Kistler dynamometer. Engineering strain calculations within this work are compliance corrected.

### 2.3. Ultrasonic-assisted compression – Transient test

To provide a basis for the expected softening effect for these alloys, a transient ultrasonic application was first tested. AA2024-O samples with dimensions of 2.27 mm and 1.60 mm in diameter and height, respectively, were compressed using a constant cross head speed of 0.007 mm/s. At roughly 0.04 mm travel, the vibrations were switched on for the remainder of the test. The total displacement was set to 1.02 mm.

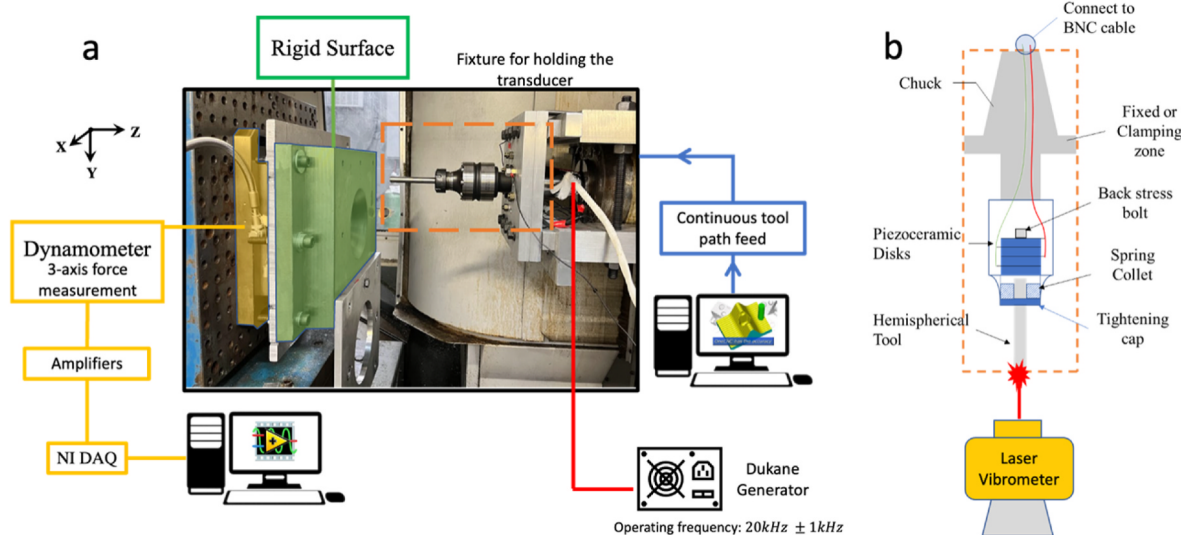


**Fig. 1.** Experimental setup. a) CNC machine which applies coupons are compressed against a rigid surface. The ultrasonic transducer is highlighted in the orange dotted box. b) schematic of the internal parts in the transducer housing. (For interpretation of the references to colour in this figure legend, the reader is referred to the Web version of this article.)

Samples were compressed with increasing ultrasonic amplitudes ranging from 0.63 μm to 5.36 μm. The final specimen height was measured after unloading and the plastic strain was calculated accordingly.

#### 2.4. Ultrasonic-assisted compression – Full UA

Ultrasonic vibrations were applied for the full compression loading of AA2024-O and AA7075-O samples listed in Table 1 (Appendix). Samples are first loaded to a rough load of 200–250 N and then vibrations were switched on for the remainder of the compression test. The acquired compression force is converted to engineering stress and strain and compliance corrected. Results for the softening magnitude were taken from a strain of 0.15. The displacement rate of 0.007 mm/s was maintained for this set of experiments as well. The strain hardening rate was calculated for full UA compression tests defined by:

$$\dot{\varepsilon} = \frac{d\varepsilon}{dt} \quad (6)$$

#### 2.5. Full application of ultrasonic vibrations – modified specimen dimensions

Samples of AA2024-O and AA7075-O dimensions were varied according to Table 1. Ultrasonic vibrations were switched on at a similar compression force of 200–250 N and allowed to run for the remainder of the test. The results are plotted in terms of engineering stress and strain. Acoustic softening results presented in this work were calculated at an engineering strain of 0.15 unless stated otherwise.

### 3. Results and discussion

#### 3.1. Transient application of vibrations

The stress strain curve during the transient application of ultrasonic vibrations on AA2024-O specimens is shown in Fig. 2. The initial loading period up to 0.2 strain is the quasi-static loading without any ultrasonic assistance. The transducer was activated at approximately 0.20 strain. The vibration was switched off during the unloading portion of the test. As the vibration amplitude increases from 0.63 μm to 5.36 μm, the softening magnitude increases from 14.4% to 66.1% respectively. The softening magnitude is commonly compared to the applied vibration amplitude as shown in Fig. 3a. A linear relationship to the applied

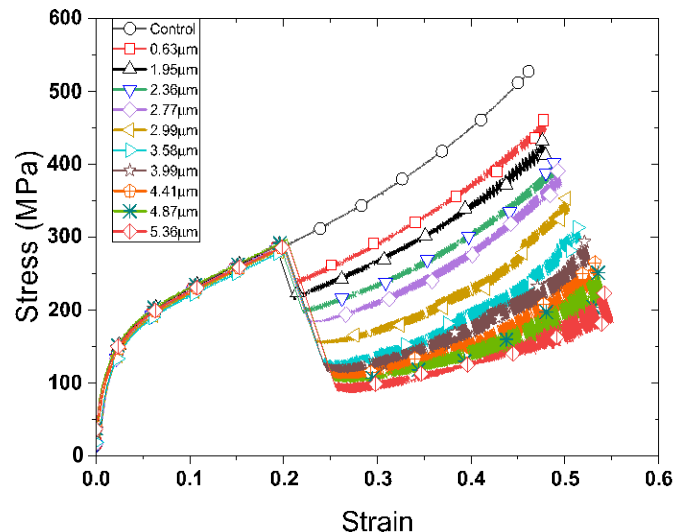


**Fig. 2.** Compression of AA2024-O coupons at various ultrasonic vibration amplitudes.

amplitude was found for AA2024-O material. The unloaded specimen height was measured to characterize the plastic strain. The results, in Fig. 3b, indicates higher plastic deformation of compressed samples with increasing vibration amplitude. The results can be compared to similar load or displacement-controlled experiments in literature. Sui et al. [23] conducted load control indentation tests and found larger deformation areas when adding ultrasonic assistance. Lum et al. [24] performed load and displacement-controlled biaxial bonding of gold and found higher plastic strains with increasing amplitudes. Given the known compliance of the system and cross head travel, the sample spring-back was back calculated and shown to decrease with increasing amplitude. This coincides with the proposed dislocation annihilation mechanism in acoustic softening leading to a reduction in stored defect energy and thus, less resistance to slip. This effect can be observed right at the start of adding the vibrations. The drop in stress shows the elastic deflection of the platen which would imply an immediate increase in the strain of the sample.

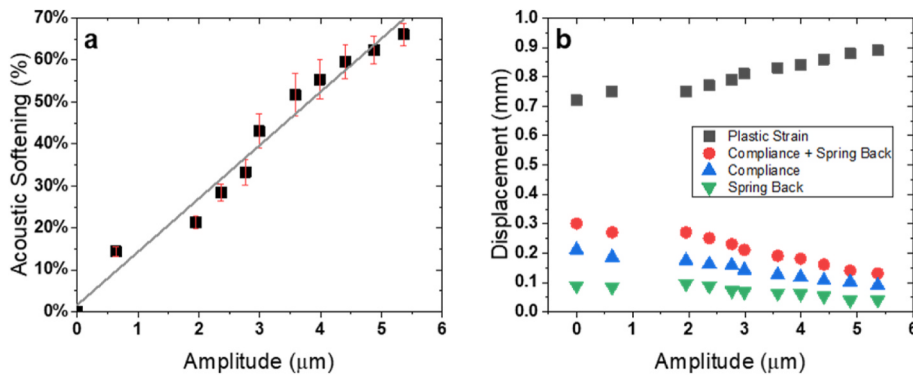


Fig. 3. a) Acoustic softening calculated from compression testing of AA2024-O coupons. b) System compliance, plastic deformation, and sample springback compared to the applied amplitude.

### 3.2. Full application of ultrasonic vibrations

AA2024-O specimens were first loaded to an applied force of 200–250 N from which vibrations were applied for the remainder of the test. The engineering stress and strain are plotted in Fig. 4a for vibration amplitudes of 0.63  $\mu\text{m}$ , 2.99  $\mu\text{m}$ , and 4.87  $\mu\text{m}$ . Like the transient application of UA, the softening effect has a positive correlation to amplitude. The softening ratio plotted in Fig. 4b is based on Eq. (1). At initial strains, the softening effect is maximum and decreases as the sample is strained further. Since acoustoplasticity is known to change the resulting microstructure, potentially leaving a residual hardening or softening effect, a similar argument can be made about the specimen state of strain influencing the softening magnitude. During the early stages of strain, the material deforms through multiflipping and resembles a dislocation forest like defect structure. At higher strains, these dislocations coalesce into energy defect structures such as subgrains which has been documented in the deformation of aluminum using UA [23]. The results suggest the internal defect structure at higher strains benefits less from the acoustic softening phenomenon or possibly impeding the effect because of higher attenuation.

The strain hardening rate, Fig. 5, of the control sample and 0.63  $\mu\text{m}$  sample are similar. Raising the amplitude to 2.99  $\mu\text{m}$  shows a slight decrease in the strain hardening rate and an even greater decrease with the 4.87  $\mu\text{m}$  sample. Most literature reports do not specify the strain hardening rate during UA, however, the work of Zhou et al. [7] provides insight into residual effects after turning vibrations off. Zhou performed UA compression tests on commercially pure aluminum with an amplitude of 4.65  $\mu\text{m}$  for different times and strain durations. The work showed residual hardening is possible after 24 s or roughly  $\Delta \epsilon = 0.093$  strain. Shorter times with UA excitation showed no changes in residual hardening and longer times led to greater hardening effects. Therefore, depending on either the duration or strain under UA, the internal defect structure becomes distinct from the quasi-static loading sample. Based on the work of Yao et al. [13], the lower strain hardening behavior

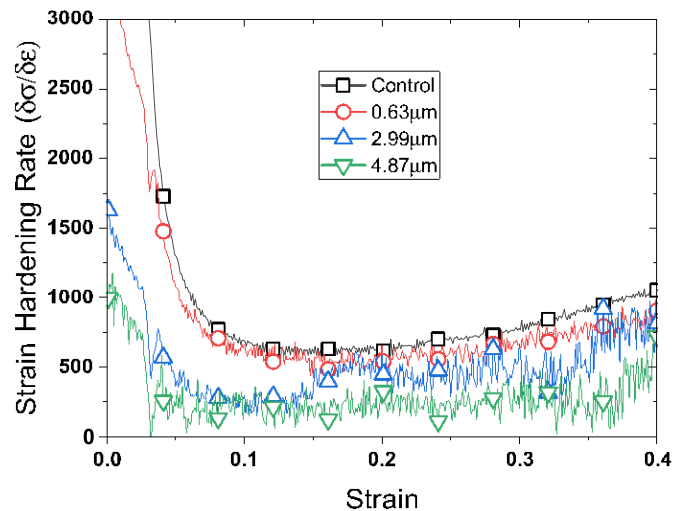


Fig. 5. Strain hardening rate of full ultrasonic assisted compression specimens.

shown in Fig. 5 is a combination of less dislocation generation and more facilitation of dislocation annihilation. To make claims on permanent differences in dislocation structure and density, microscopy techniques that delineate the differences in statistically stored dislocations are needed.

### 3.3. Effect of specimen volume on acoustic softening

AA2024-O and AA7075-O compression specimens were cut to a variety of dimensions listed in Table 1. Full UA application was implemented for these tests. The acoustic softening magnitude,  $\Delta\sigma$ , was calculated at a strain of 0.15 and plotted in Fig. 6 for comparison. In all

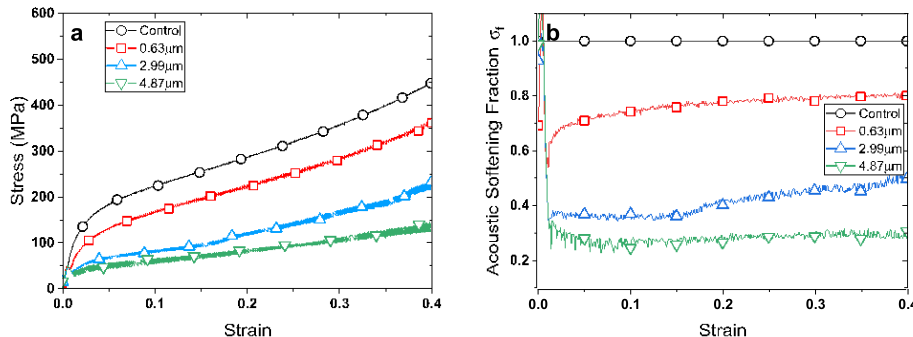


Fig. 4. Full ultrasonic assisted compression of AA2024-O. a) Stress-strain curve and b) the corresponding acoustic softening fraction at those amplitudes.

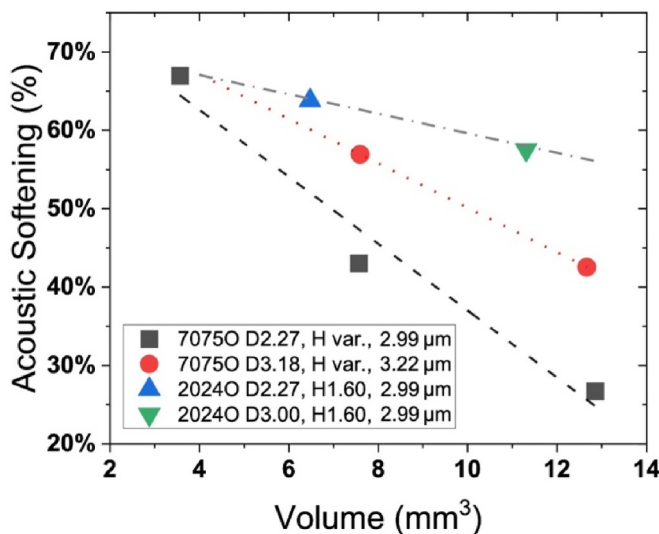


Fig. 6. Ultrasonic assisted compression of AA2024O and AA7075O alloys grouped by their dimensions and volumes.

cases, a reduction in specimen volume resulted in a greater softening response. This reaffirms the initial results reported by Zhou [4]. Increasing the vibration amplitude from 2.99 μm to 3.22 μm, increased the softening effect for the same volume as expected.

Given the influence vibrations have on friction conditions, termed surface effects, the results for the 3.18 mm diameter AA7075-O sample could be exhibiting greater softening due to lower friction conditions [3]. To demonstrate the impact of a change in diameter, two AA2024-O samples of the same height and different diameters were tested. The larger diameter sample showed a smaller softening magnitude. Thus, the higher softening response for the 3.22 μm data set are primarily driven by softening in the bulk of the sample.

Based on the trendline from Fig. 3a, increasing the vibration amplitude from 2.99 μm to 3.22 μm should improve the softening effect by roughly 5.0%. When comparing the response for the AA7075-O alloy in Fig. 6, the softening improved 15.8% under equivalent sample volume of 12.5 mm<sup>3</sup>. As the sample volume decreases, the trendlines between the 2.99 μm and 3.22 μm data sets appear to converge instead of being equidistant. From an energy perspective, as the sample volume decreases, the acoustic energy density reaches a critical point which defines an upper limit of acousto-plasticity. The softening response of these sample sets are plotted relative to common acoustic parameters such as acoustic energy, intensity, or stress based on Eqs. (3)–(5). The acoustic energy density and acoustic stress, Fig. 7a and b respectively, are invariant to the changes in sample dimensions as indicated by a vertical trend. The acoustic intensity was not plotted here because the results

would be similar to acoustic energy density as  $E\lambda^2$ . This is a possible explanation for large variations in acoustic softening reported in literature. For example, Yao [13] observed softening percentages up to 35% with a 2 μm amplitude while Aziz [25] required an amplitude of 20 μm to achieve 32% softening. Their commercially pure aluminum samples heights were 2 mm and 8 mm for Yao and Aziz experiments respectively [13,25]. Although their samples may differ in microstructure, the sample set presented in this work were machined from the same sheet. The main difference that defines a greater response is the sample dimensions. Here, we propose a parameter called amplitude strain which accounts for changes in the specimen height during compression testing. The amplitude strain is represented in Eq. (7):

$$\lambda_e = \frac{\lambda}{h_e} \quad (7)$$

where the amplitude strain  $\lambda_e$  is the applied amplitude  $\lambda$  divided by the height of the specimen  $h_e$  at a given strain. The  $\lambda$  parameter, calculated at a specimen strain of 0.15, was plotted in Fig. 8 and showed a linear fit across sample sets of different dimensions. The results were further divided into their respective alloys in Fig. 9a and it is evident a close correlation. Incorporating the strain of the specimen is necessary based on Fig. 9b. As the material stores more internal defects, the microstructure provides the beneficial effects of acousto-plasticity. This trend was found to be true for the 0.63 μm and 4.87 μm samples as well; however, the spread in response was not as large as the 9% difference in

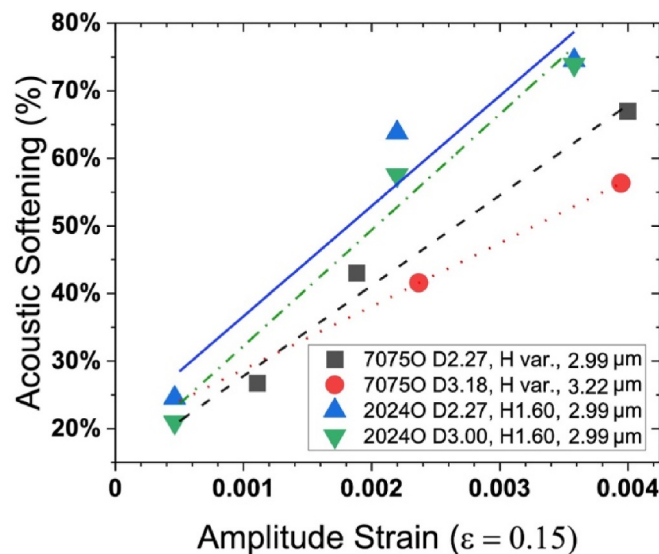


Fig. 8. Acoustic softening response compared to the amplitude strain parameter.

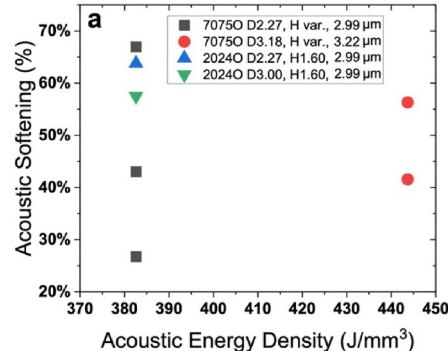
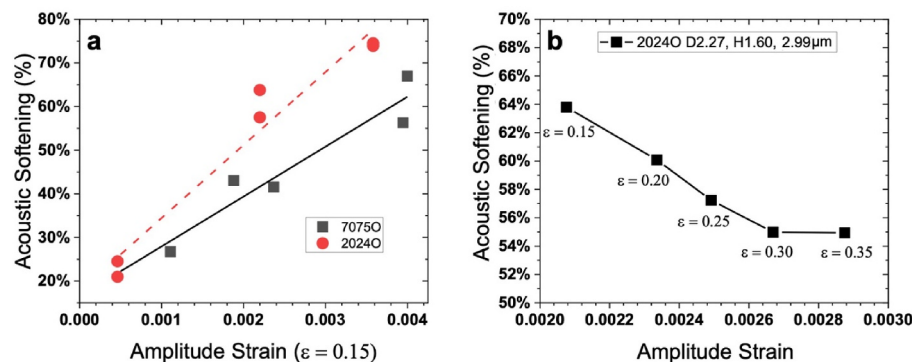


Fig. 7. Acoustic softening of AA2024-O and AA7075-O specimens at 0.15 strain. a) acoustic energy density (refer to Eq. (3)) and b) acoustic stress (refer to Eq. (5)).



**Fig. 9.** Ultrasonic assisted compression of AA2024O and AA7075O alloys. a) grouping based on alloy type. b) acoustic softening percent calculated at different engineering strains from a AA2024-O full ultrasonic assisted compression test.

**Fig. 9b.** AA2024-O samples with 0.63  $\mu$ m and 4.87  $\mu$ m applied amplitudes both showed a spread of  $\sim 5\%$  comparing values at 0.15 and 0.35 strain. An interesting aspect to note is the non-zero Y-intercept when extrapolating the results in **Fig. 6**. This deviates from the trend in **Fig. 3a**. A simple explanation would be that the trend is not linear but instead asymptotic where the softening converges towards 0 as the amplitude strain approaches 0. Frictional effects at low amplitude strains may contribute to a non-zero intercept extrapolation. Finally, the deviation from the trend in **Fig. 6** might be due to changes in internal microstructure as the vibration assistance was applied for the full duration of the compression test. This observation requires further study.

As shown in **Fig. 8a**, AA7075-O has a inherently lower slope compared to AA2024-O material which can be due to multiple reasons. First, Ahmad et al. [13] performed equal-channel angular press on commercial pure aluminum with different grain size and observed a direct correlation between softening and grain size. To characterize the grain size, both alloys were ground, polished, and electrolytically etched using a Barker's reagent. **Fig. 10a** and b represent the transverse direction | normal direction micrographs of the AA2024-O and AA7075-O under polarized light. Qualitatively, the grains in the AA2024-O sample are larger than the AA7075-O alloy. The histograms of grain length along the normal direction (**Fig. 10c**) and the transverse direction

(**Fig. 10d**) support the visual micrographs. Additional information on the texture of the two alloys can be found in the Appendix, **Fig. 12**.

A second factor is the precipitate microstructure in these age hardenable alloys. The secondary electron micrographs in **Fig. 11** suggest a higher density and finer precipitates in the AA7075-O alloy. In addition to nucleated precipitates, solute remaining in the matrix contribute to solute strengthen. Given the difficulty in quantifying and controlling the precipitate characteristics, there have not been experimental studies in literature to the authors knowledge. Investigation of the acoustic softening behavior in AA7075 at different heat-treated stages would be impactful as the alloy is commonly deformed right after softening, in the W temper state, followed by a quench and precipitation heat treatment.

#### 3.4. Incorporating amplitude strain in existing acoustoplasticity models

Results from **Fig. 6** supports the notion of higher acoustic energy input leading to greater softening effects. However, the variance in acoustic energy density and stress terms imply that the terms are not representative, and that softening is driven by another experimental factor: amplitude strain  $\lambda_\varepsilon$ . This new finding suggests that the softening effect is directly related to the amplitude strain and provides some

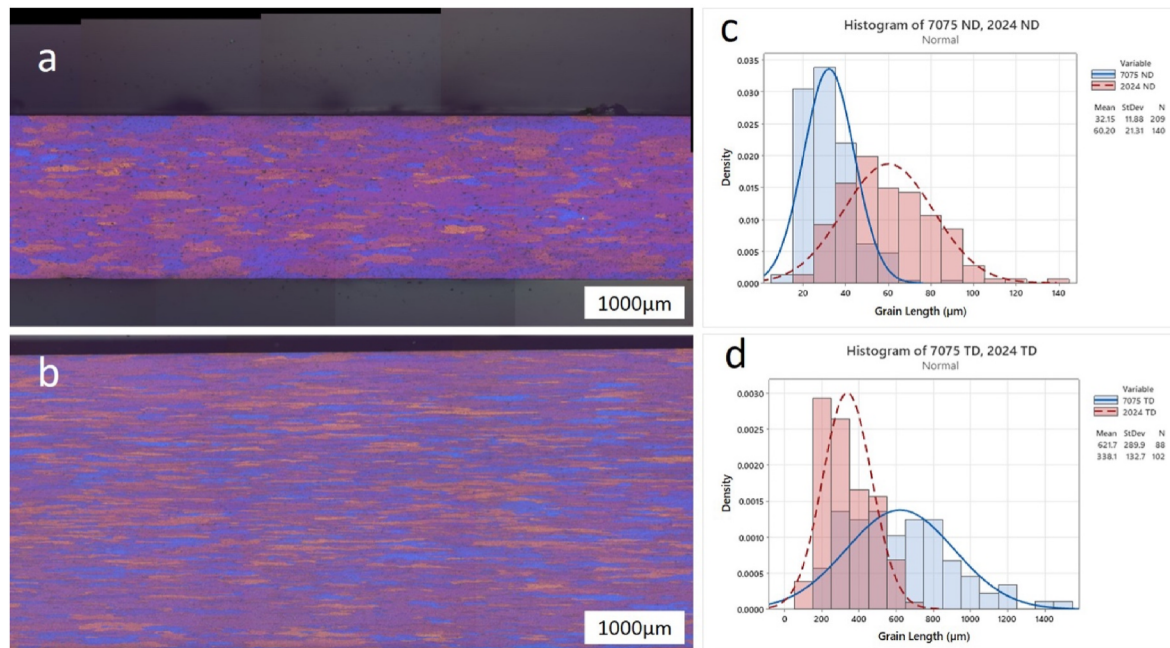


**Fig. 10.** Barker's etched micrographs of a) AA2024-O and b) AA7075-O. Histograms of grain length in the c) normal direction and d) transverse direction.

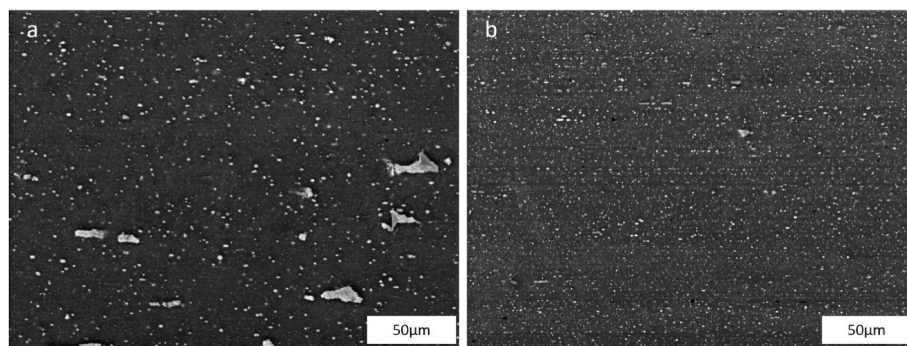


Fig. 11. Secondary electron micrographs of a) AA2024-O and b) AA7075-O.

clarify on the wide range of softening responses reported in literature. This amplitude strain component can be incorporated in crystal plasticity and dislocation evolution models commonly used in the community. Yao used a dislocation density model and introduced a stress reduction ratio  $\Delta\lambda$  [13]:

$$\Delta\lambda = \frac{(\lambda - \lambda_e)^m}{\theta \tau} \quad (8)$$

where  $\tau$  is the critical resolved shear stress required for slip,  $E$  is the acoustic energy density (Eq. (3)), and  $\theta$  and  $m$  are experimental fitted parameters. Based on the UAC experiments, a value of 0.5 was fitted for  $m$  which suggests a linear correlation to amplitude. To obtain the shear stress under ultrasonic assisted conditions:

$$\tau_{UA} = \tau[1 - \lambda] = \tau[1 - (\chi \cdot \lambda_e + C)] \quad (9)$$

where  $\chi$  refers to the slope of the amplitude strain plot in Fig. 8,  $\lambda_e$  is the amplitude strain parameter and  $C$  represents the y-intercept.  $\lambda$  is equal to  $\chi \cdot \lambda_e$ . Yao et al. [13] further back extrapolated the dislocation storage and annihilation coefficient in the MK model to obtain the physical phenomenon of plasticity relationship.

In crystal plasticity models, the critical resolved shear stress is modified to represent softening by the shear strain rate equation [14,15]:

$$\dot{\gamma}^\alpha = \dot{\gamma}^0 \operatorname{sgn}(\tau^\alpha) \frac{\tau^\alpha}{\tau^\alpha + U_{soft}} \quad (10)$$

$\dot{\gamma}^0$  is the pre-exponential factor or frequency factor,  $\tau^\alpha$  is the resolved shear stress on a slip plane,  $\tau^\alpha$  is the critical resolved shear stress, and  $U_{soft}$  is the acoustic softening parameter. Similarly represented the  $U_{soft}$  by:

$$U_{soft} = (1 - d_{ut} \cdot I_{ultrasonic})^{e_{ut}} \quad (11)$$

$d_{ut}$  and  $e_{ut}$  are experimental fit parameters and  $I_{ultrasonic}$  is the acoustic intensity (Eq. (4)). Similarly,  $d_{ut} \cdot I_{ultrasonic}$  can be replaced by  $\lambda$ .

Apart from reducing the activation energy required for slip, others have suggested a change in the pre-exponential factor  $\dot{\gamma}^0$  or the bypass attempt frequency to be significant in driving the acoustic softening effect [7,16]. Sui et al. [26] and Cheng et al. [27] modeled the acoustic softening response using dislocation dynamics (DD) simulation and suggested that during the unloading portion of the vibration, dislocations are allowed to travel in reverse motion spurred by the relieved stress and dislocation-dislocation interactions. Under combined forward and reverse motion, the dislocations are interacting with complementary dipoles for annihilation or allowed to cross slip in search of annihilation sites. Considering this framework of reactive strain as the driver of softening magnitude, the necessity of using efficiency and compensation coefficients in more complex ultrasonic assisted forming processes arise from variability in amplitude strain distribution. Plastic forming and incremental forming, demonstrated by the models from

Sedaghat, have inherent strain gradients and a distribution of  $\lambda_e$  in each element [22]. Further work on modeling deformation processes with a strain and  $\lambda_e$  distribution is worthwhile.

#### 4. Conclusion

Two aluminum alloys, AA2024-O and AA7075-O were compressed using ultrasonic assistance. The effect of specimen volume and dimensions were investigated in this study and the implications on complex forming processes was discussed. The findings of this work are summarized:

- Acoustic softening magnitude correlates linearly with the applied vibration amplitude for AA2024-O and AA7075-O materials.
- Plastic strain increases and springback decreases with higher applied amplitudes.
- Reducing the specimen height and volume while maintaining the same applied amplitude results in a higher acoustic softening response.
- Acoustic energy, intensity, and stress terms are invariant to changes in specimen height. Instead, amplitude strain  $\lambda_e$  is required to accurately represent these differences in response.

#### CRedit authorship contribution statement

**Randy Cheng:** Conceptualization, Methodology, Investigation, Formal analysis, Visualization, Writing – original draft. **Scott Rose:** Conceptualization, Writing – review & editing. **Alan Taub:** Conceptualization, Methodology, Formal analysis, Supervision, Writing – review & editing.

#### Declaration of competing interest

The authors declare that they have no known competing financial interests or personal relationships that could have appeared to influence the work reported in this paper.

#### Data availability

Data will be made available on request.

#### Acknowledgements

The authors would like to acknowledge the National Science Foundation (CMMI No. 1841755), the Boeing Company for their technical support, and Professor Xun Liu and Dr. Jianfu Kang from The Ohio State University for their valuable discussions with regards to the data presented here and the relevant literature.

## Appendix

**Table 1**

Compression specimen dimensions

Aflumfinum Aflloy	Test(s)	Diameter (mm)	Height (mm)	Amplitude (μm)	Volume (mm <sup>3</sup> )
7075-O	Volume Effect & Amplitude Strain	2.27	3.18	2.99	12.85
		2.27	3.18	2.99	12.85
		2.27	1.87	2.99	7.57
		2.27	1.87	2.99	7.57
		2.27	0.88	2.99	3.56
		3.18	1.62	3.22	12.85
		3.18	1.62	3.22	12.85
		3.18	1.62	3.22	12.85
		3.18	0.96	3.22	7.61
		3.18	0.96	3.22	7.61
2024-O	Volume Effect & Amplitude Strain	2.27	1.6	0.63	6.48
				2.99	6.48
				4.87	6.48
		3		0.63	11.31
				2.99	11.31
				4.87	11.31
		2.27	1.6	0.63	6.48
				1.95	6.48
				2.36	6.48
				2.77	6.48
Intermittent application of ultrasonic vibrations	Intermittent application of ultrasonic vibrations			2.99	6.48
				3.58	6.48
				3.99	6.48
				4.41	6.48
				4.87	6.48
				5.36	6.48

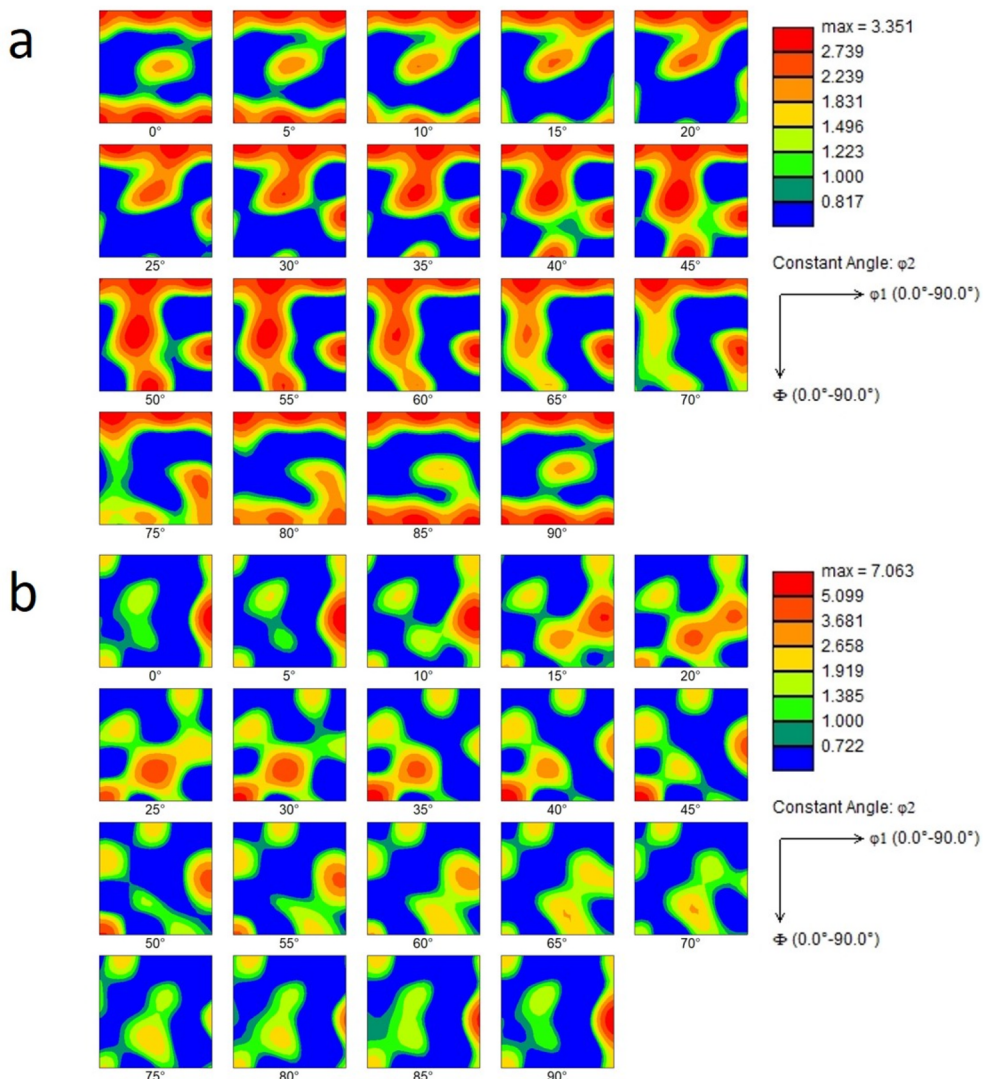


Fig. 12. Orientation distribution function of a) AA2024-O and b) AA7075-O textures.

## References

- [1] F. Blaha, B. Langencker, Tensile deformation of zinc crystal under ultrasonic vibration, *Naturwissenschaften* 42 (1955) 1–10.
- [2] J. Kang, X. Lifu, M. Xu, Plastic deformation of pure copper in ultrasonic assisted micro-tensile test, *Mater. Sci. Eng. 785* (April) (2020), 139364, <https://doi.org/10.1016/j.msea.2020.139364>.
- [3] Y. Daud, M. Lucas, Z. Huang, Modelling the effects of superimposed ultrasonic vibrations on tension and compression tests of aluminiun, *J. Mater. Process. Technol.* 186 (1–3) (2007) 179–190, <https://doi.org/10.1016/J.JMATPROTEC.2006.12.032>.
- [4] Y. Daud, M. Lucas, Z. Huang, Superimposed ultrasonic oscillations in compression tests of aluminiun, *Ultrasonics* 44 (2006) e511–e515.
- [5] V. Fartashvand, A. Abduljalil, S.A. Sadough Vanfifi, Investigation of Ti-6Al-4V alloy acoustic softening, *Ultrason. Sonochem.* 38 (2017) 744–749.
- [6] Y. Lifu, C. Wang, R. Bfi, Acoustic residual softening and microstructure evolution of Ti2 copper foil in ultrasonic vibration assisted micro-tension, *Mater. Sci. Eng., A* 841 (2022), 143044.
- [7] H. Zhou, H. Cui, Q.H. Qin, Influence of ultrasonic vibration on the plasticity of metals during compression process, *J. Mater. Process. Technol.* 251 (November 2016) 146–159, <https://doi.org/10.1016/j.jmatprote.2017.08.021>.
- [8] J. Lifu, J. Li, T. Lifu, Z. Xie, L. Zhu, Y. Wang, Y. Guan, Investigation on ultrasonic vibration effects on plastic flow behavior of pure titanium: constitutive modeling, *J. Mater. Res. Technol.* (2020), <https://doi.org/10.1016/J.JMRT.2020.03.017>.
- [9] R.K. Dutta, R.H. Petrov, R. Delflez, M.J.M. Hermans, I.M. Richardson, A.J. Böttger, The effect of tensile deformation by in situ ultrasonic treatment on the microstructure of flow-carbon steel, *Acta Mater.* 61 (5) (2013) 1592–1602, <https://doi.org/10.1016/j.actamat.2012.11.036>.
- [10] T. Wen, L. Wefi, X. Chen, C.L. Pefi, Effects of ultrasonic vibration on plastic deformation of AZ31 during the tensile process, *Int. J. Mater. Metall. Mater.* 18 (2011) 70–76.
- [11] A. Deshpande, K. Hsu, Acoustic energy enabled dynamic recovery in aluminum and its effects on stress evolution and post-deformation microstructure, *Mater. Sci. Eng., A* 711 (2018) 62–68, <https://doi.org/10.1016/J.MSEA.2017.11.015>.
- [12] C.J. Wang, Y. Lifu, B. Guo, D.B. Shan, B. Zhang, Acoustic softening and stress superposition in ultrasonic vibration assisted uniaxial tension of copper foil: experiments and modelling, *Mater. Des.* 112 (Supplement C) (2016) 246–253, <https://doi.org/10.1016/j.matdes.2016.09.042>.
- [13] Z. Yao, G.-Y. Kfim, Z. Wang, L. Fafidley, Q. Zou, D. Mefi, Z. Chen, Acoustic softening and residual hardening in aluminum: modelling and experiments, *Int. J. Plast.* 39 (2012) 75–87, <https://doi.org/10.1016/J.IJPLAS.2012.06.003>.
- [14] A. Siddiqi, T. El Sayed, A thermomechanical crystal plasticity constitutive model for ultrasonic consolidation, *Comput. Mater. Sci.* 51 (1) (2012) 241–251, <https://doi.org/10.1016/J.COMMATSCL.2011.07.023>.
- [15] A. Siddiqi, T. El Sayed, Ultrasonic-assisted manufacturing processes: variational model and numerical simulations, *Ultrasonics* 52 (2012) 521–529.
- [16] K.W. Sfu, H. Lifu, A.H.W. Ngan, A universal law for metallurgical effects on acoustoplasticity, *Materiaffia* 5 (2019), 100214.
- [17] F. Ahmadfi, M. Farzani, M. Mandegari, Effect of grain size on ultrasonic softening of pure aluminum, *Ultrasonics* 63 (2015) 111–117, <https://doi.org/10.1016/J.ULTRAS.2015.06.015>.
- [18] J. Kang, X. Lifu, S.R. Nfiezgoda, Crystal plasticity modelling of ultrasonic softening effect considering anisotropy in the softening of slip systems, *Int. J. Plast.* 156 (May) (2022), 103343, <https://doi.org/10.1016/j.fijpflas.2022.103343>.
- [19] M. Vahdati, R. Mahdavinejad, S. Amiri, Investigation of the ultrasonic vibration effect in incremental sheet metal forming process, in: *Proceedings of the Institution*

of Mechanical Engineers, Part B: Journal of Engineering Manufacture, 2017, <https://doi.org/10.1177/0954405415578579>.

[20] R. Cheng, N. Wifley, M. Short, X. Lfui, A. Taub, Applying ultrasonic vibration during single-point and two-point incremental sheet forming, *Procedia Manuf.* 34 (2019) 186–192, <https://doi.org/10.1016/J.PROMFG.2019.06.137>.

[21] S. Abdul Aziz, M. Lucas, The effect of ultrasonic excitation in metal forming tests, *Appl. Mech. Mater.* 24–25 (2010) 311–316.

[22] H. Sedaghat, W. Xu, L. Zhang, Ultrasonic vibration-assisted metal forming: constitutive modelling of acoustoelasticity and applications, *J. Mater. Process. Technol.* 265 (2019) 122–129, <https://doi.org/10.1016/J.JMATPROTEC.2018.10.012>.

[23] K.W. Sfu, A.H.W. Ngan, I.P. Jones, New insights on acoustoelasticity – ultrasonic vibration enhances subgrain formation during deformation, *Int. J. Plast.* 27 (5) (2011) 788–800, <https://doi.org/10.1016/J.IJPLAS.2010.09.007>.

[24] I. Lum, H. Huang, B.H. Chang, M. Mayer, D. Du, Y. Zhou, Effects of superimposed ultrasound on deformation of gold, *J. Appl. Phys.* (2009), <https://doi.org/10.1063/1.3068352>.

[25] A. Aziz, Characterising the Effective Softening in Ultrasonic Forming of Metals, 2012, <http://theses.gla.ac.uk/3704/>.

[26] K.W. Sfu, A.H.W. Ngan, Understanding acoustoelasticity through dislocation dynamics simulations, *Philos. Mag. A* 91 (2011) 4367–4387.

[27] B. Cheng, H.S. Leung, A.H.W. Ngan, Strength of metals under vibrations – dislocation-density-function dynamics simulations, *Philos. Mag. A* 95 (16–18) (2015), <https://doi.org/10.1080/14786435.2014.897008>.